Environmental Science & Technology

Article

Cite This: Environ. Sci. Technol. 2018, 52, 40−51

pubs.acs.org/est

# Biodegradation of Carbon Nanotube/Polymer Nanocomposites using a Monoculture

David G. Goodwin, Jr.,[†] Iruhany Boyer,[‡] Thomas Devahif,[§] Cong Gao,[∥] Benjamin P. Frank,[†] Xier Lu,[⊥] Leo Kuwama,[†] Tucker B. Gordon,[†] JingJing Wang,[#] James F. Ranville,[#] Edward J. Bouwer,[⊥] and D. Howard Fairbrother*[,†]

[†]Department of Chemistry, Johns Hopkins University, Baltimore, Maryland 21218, United States

[‡]Centro de Química, Instituto Venezolano de Investigaciones Cientificas (IVIC), Altos de Pipe, Caracas 1020-A, Miranda Venezuela

[§]Department of Chemistry, University of Namur, B-5000, Namur, Belgium

[∥]College of Chemistry, Jilin University, Changchun, 130012, China

[⊥]Department of Environmental Health and Engineering, Johns Hopkins University, Baltimore, Maryland 21218, United States

[#]Department of Chemistry and Geochemistry, Colorado School of Mines, Golden, Colorado 80401, United States

Supporting Information

**ABSTRACT:** The biodegradation rates of carbon nanotube (CNT)/ polymer nanocomposites (PNCs) containing poly-ε-caprolactone (PCL) were investigated using *Pseudomonas aeruginosa*, a microorganism commonly found in the environment. CNT/PCL nanocomposite mass loss profiles revealed that the rate of PCL matrix biodegradation decreased systematically as the CNT loading increased from 0.1 to 10% w/w. Addition of even a low CNT loading (<1% w/w) caused the CNT/PCL biodegradation rate constant to decrease by more than 50%. Similar trends in biodegradation rate were observed for both pristine and oxidized multiwall CNTs embedded in PCL. During PCL matrix biodegradation, CNT accumulation was observed at the surface of CNT/PCL nanocomposites and single particle inductively coupled-mass spectrometry experiments revealed no measurable CNT release to the culture fluid. Experimental data indicated that biodegradation proceeded as a result of biofilm formation on the CNT/PCL nanocomposites and decreased as a function of CNT loading due to the cytotoxicity of CNTs toward *P. aeruginosa* and the physical barrier presented by the surface-accumulated CNTs to the underlying PCL substrate. As the CNT loading in the CNT/PCL nanocomposites increased, the microbial proliferation of planktonic cells in the surrounding media also decreased as did the biodegradation rate of PCL samples present in the same reactors. Results from this study demonstrate that the inclusion of CNTs into polymer matrices could increase the environmental persistence of polymers in lakes, landfills, and surface waters.

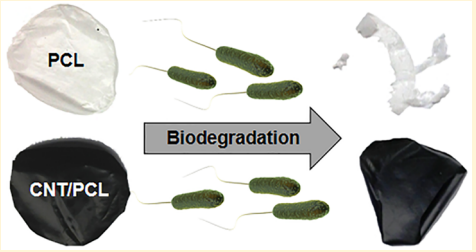


## INTRODUCTION

The incorporation of carbon nanotubes (CNTs) into polymer matrices at low mass fractions, typically (1−5)% w/w, can produce CNT/polymer nanocomposites (CNT/PNCs) with enhanced polymer properties such as tensile strength, elastic modulus, thermal stability, and electrical conductivity.[1−3] Thus, CNTs have already been incorporated into a range of commercially available products that include antistatic packaging, windmill turbines, fuel tank linings, sporting equipment, and biomedical implants and devices.[1,3−5]

With the expanding use of CNTs in products, the environmental impact of CNT-containing polymer waste warrants investigation. Similar to conventional plastics, CNT/PNCs are likely to end up in landfills, surface waters, and wastewater treatment plants following consumer use.[6,7] At this stage in the life cycle, the ultimate fate and persistence of polymeric materials is strongly influenced by microbial interactions that can lead to biodegradation. Biodegradation involves enzymatic scission of polymer chains to lower molecular weight products and eventually to small molecules such as $CO_2$, $CH_4$, and water.[8] The kinetics of biodegradation for different polymers can range from a few days to several hundred years and depend on material type, crystallinity, tacticity, molecular weight, and the presence of fillers.[9] Polymer biodegradation can proceed under either aerobic or anaerobic conditions by using oxygen or an alternative electron acceptor, respectively, to achieve respiration.[10,11] Under aerobic conditions, polymers are generally considered biodegradable if they are >60% mineralized by microorganisms to $CO_2$ within 180 days.[12,13]

Many petroleum-based polymers, such as polyethylene, do not contain functional groups that can be easily transformed by enzymes, and are therefore recalcitrant to biodegradation.

Received: April 21, 2017
Revised: November 16, 2017
Accepted: November 21, 2017
Published: November 21, 2017






DOI: 10.1021/acs.est.7b02062
Environ. Sci. Technol. 2018, 52, 40−51

Nevertheless, microorganisms can eventually degrade these biologically inert polymers in tandem with abiotic environmental processes such as acid rain, hydrolysis, and photodegradation since these processes can cause polymer oxidation and chain scission, which can facilitate biodegradation.[8,14−16]

A small number of petroleum based polymers, such as polybutylene succinate (PBS) and poly-ε-caprolactone (PCL), can biodegrade on a short time scale (days, months).[17−19] Other types of biodegradable polymers are those that can be derived cheaply from plants, microorganisms, and fungi (e.g., starch, polyhydroxyalkanoates, chitosan, etc.). One common attribute of biodegradable polymers is that they oftentimes require fillers,[20,21] such as nanoclays,[22,23] graphite oxide,[24] graphene oxide,[25] and CNTs[26] in order to exhibit the necessary materials properties (e.g., mechanical strength) and functionality required for commercial applications. In some instances, the impact of these nanofillers on biodegradation or enzymatic decomposition of polymers has been studied.[22−24] For example, the addition of nanoclay or graphite oxides fillers has been shown to enhance the biodegradation or enzymatic decomposition rate of polymers.[24,27] This has been attributed to an increase in the number of amorphous zones formed at the interface of the filler and the polymer matrix.[27] These amorphous zones do not cause a significant change in the fraction of crystallinity but often contain hydroxyl groups which promote enzymatic hydrolysis.[23,28,29] In contrast to nanoclays and graphite oxide, the effect of adding CNTs to biodegradable polymers remains unclear. As fillers, CNTs are not expected to biodegrade readily in the presence of microorganisms, since even under aggressive, abiotic conditions, they can only partially degrade.[30−32] Moreover, CNTs at the surface of CNT/PNCs have been shown to be cytotoxic to a variety of different microorganisms (e.g., *Pseudomonas aeruginosa*, *Escherichia coli*, and *Bacillus subtilis*) when direct contact occurs between CNTs and microorganisms.[33−36] The antimicrobial properties associated with CNTs have been shown to retard but not prevent biofilm formation, a common precursor to polymer biodegradation.[37] Thus, cytotoxicity could have a significant effect on biodegradation rates. For example, Fan et al. showed that another nanofiller, graphene oxide, reduced the biodegradation of chitosan as a result of graphene oxide cytotoxicity at 0.25% w/w and 0.60% w/w mass loadings.[25]

In the present study, both pristine multiwall CNTs (MWCNTs) and oxidized MWCNTs (O-MWCNTs) were incorporated into PCL at varied CNT loadings (0−10% w/w). MWCNTs were chosen since they are most commonly used in commercial products, principally due to their lower cost as compared to single-wall CNTs.[3] PCL was selected as the biodegradable polymer matrix since its mechanical and thermal properties are known to be enhanced by the inclusion of CNTs.[38−40] Furthermore, we have previously studied biofilm formation on PCL and CNT/PCL surfaces.[41] CNT/PCL nanocomposites were biodegraded aerobically using a monoculture of *P. aeruginosa*. *P. aeruginosa* was selected as the microorganism in this study since it is commonly found in water supplies and soils, is versatile in polymer biodegradation processes, and is representative of many types of Gram negative bacteria.[11,42] Furthermore, bioremediation via augmentation and industrial waste treatment can rely on individual taxa, such as *P. aeruginosa*.[43,44] Although mixed culture conditions are more representative of the environment, monoculture studies provide better control over microbial type and population, which in turn leads to more consistent biodegradation trends as seen previously in PCL biodegradation studies using monocultures of *Alcaligenes faecalis*, *Paecilomyces lilacinus*, and *Acinetobactercal coaceticus* var. *lwojji*.[29,45,46]

To date, the impact of CNT inclusion on the stability of biopolymers has been restricted to a few studies, most of which involve enzymatic decomposition. For example, pure enzymes were used to decompose both CNT/polymer nanocomposites and polymer that was covalently attached to modified MWCNTs.[26,47−50] In one study, complete PCL decomposition occurred in the presence of *Pseudomonas* lipase when PCL was grafted onto MWCNTs.[50] In terms of biodegradation rate, Singh et al. showed that a 1% mass loading of CNTs dispersed in PLA accelerated the enzymatic decomposition rate of PLA using Proteinase K.[26] This accelerated decomposition rate was attributed to a number of possible reasons including an increase in amorphous zones that were more susceptible to enzymatic hydrolysis due to functionalization or potentially higher enzyme binding to the CNTs in the polymer nanocomposite substrate.[26] In contrast, other studies have shown that MWCNTs reduce the polymer biodegradation rate.[47,48] For example, MWCNT/PCL nanocomposites containing low (0.2 and 0.5% w/w) MWCNT loadings reduced enzymatic decomposition of the PCL matrix by about 30% mass loss relative to the neat PCL control.[47] This decrease in biodegradation rate was hypothesized to be a result of degraded material and enzyme entrapment by the CNTs slowing down further decomposition.[47] Ho et al. also demonstrated that oxidized MWCNTs at 1% and 3% mass loadings systematically decreased the enzymatic decomposition rate (by *Pseudomonas* lipase) of PCL in 3D-printed tissue scaffolds.[48] Furthermore, Patangrao et al. showed that pristine MWCNTs slow down *Pseudomonas* lipase decomposition of PCL as a function of CNT loading at 1%, 2%, and 3% w/w, ascribed either to an increase in the hydrophobicity of the polymer or enzyme denaturation.[49] To date, however, no studies have investigated the degradation of MWCNT/PCL nanocomposites by monocultures as a function of CNT loading and type.

In this study we have explored the effect of CNT loading and type on PCL biodegradation in the presence of *P. aeruginosa*. Biodegradation was assessed by measuring the mass loss of CNT/PCL nanocomposites as compared to the mass loss of PCL biodegraded under the same conditions. This type of comparative mass loss measurement provides a means to determine biodegradation rates and is consistent with several international standards, including biodegradation studies of PCL and other polymers biodegraded under aerobic conditions.[9,10,12,13,45] This study sought to determine the effect of CNTs on biodegradation processes under well-defined conditions as well as the fate of CNTs in nanocomposites after biodegradation.[51,52] Overall, the relative rate of PCL biodegradation with two CNT filler types at several different mass loadings, the transformation of the nanocomposite surface, the effect of the nanocomposite on the surrounding culture, and the concentration of CNTs released during biodegradation were investigated.[53]

## MATERIALS AND METHODS

**Materials.** *i. Nanocomposite Preparation.* Oxidized MWCNTs (O-MWCNTs, Nanocyl NC700) and pristine MWCNTs (NanoLab PD15L5-20 and Southwest Nanotechnologies Inc. 7773840) are described in the SI. CNT/PCL nanocomposites were prepared by adding 16 mg of ethylcellulose (EC, 48.0−49.5% (w/w) ethoxyl basis, Lot No.


DOI: 10.1021/acs.est.7b02062
Environ. Sci. Technol. 2018, 52, 40−51

BCBG4792 V, Sigma-Aldrich), a known mass of CNTs, and 400 mg of poly-ε-caprolactone (PCL, average $M_n$ 45 000, Sigma-Aldrich) to a 50 mL Erlenmeyer flask containing 40 mL of dichloromethane (DCM, > 99.8%, Sigma-Aldrich). The EC macromolecules were used to stabilize CNTs in DCM. PCL controls (0% w/w CNTs) were prepared in the same way with 4% w/w EC. Five mL of both PCL and CNT/PCL casting solutions were slow-dried in aluminum dishes at room temperature. The dried polymer (~30 mm in diameter) was peeled from the dish to produce coupons for biodegradation studies. Further details and images of PCL and CNT/PCL nanocomposites are presented in the Supporting Information (SI) (Figure S1).

*ii. Bacterial Strain.* Prior to biodegradation experiments, 0.5 mL of *P. aeruginosa* wild type (ATC 27853) frozen stock (see details in SI) was thawed, added to 75 mL LB broth (25 g/L LB broth), and grown overnight to the stationary phase at 37 °C and 225 rpm in an incubator shaker.

*iii. PCL Triol Solution Preparation.* For biodegradation to occur on an experimentally accessible time scale, it was necessary to add PCL triol (Sigma-Aldrich, $M_n$ ~ 300, 1.07 g/mL density @ 25 °C, Lot No.: MKBT5188 V), a small molecule version of PCL, to enhance the production efficiency of PCL-degrading enzymes (i.e., lipases) by the microorganism in the media. Use of a small molecule version of PCL to increase lipase production has been employed in previous biodegradation studies using ε-caprolactone.[54,55] It is important to point out that PCL triol has the same chemical structure (Mn = 300 kDa for PCL triol versus Mn = 45 000 kDa) as the PCL in the nanocomposites, so the biodegradation process is expected to be the same for both types of PCL. The key differences are the number molecular weight and the form of the material: PCL triol is soluble in water at its low number molecular weight and is easier to access by microorganisms in this soluble-form while the PCL in the nanocomposites is in a solid, insoluble, semicrystalline form (i.e., stacked polymer chains). PCL triol solutions (3 g/L preparation described in SI) were used as the medium for *P. aeruginosa* growth. Microbial growth required shaking and aerating the PCL triol medium, a process not practical for microbial growth using larger solution volumes (>500 mL). Thus, several 500 mL PCL triol solutions were prepared for seeding by the cultures grown in LB broth; seeding is described in the next section.

**Biodegradation Experiments.** *i. Inoculation.* To grow *P. aeruginosa* in PCL triol media prior to biodegradation studies, 1 mL of stationary phase *P. aeruginosa* in LB broth was seeded into each 500 mL PCL triol medium. *P. aeruginosa* was then grown to consistent microbial concentrations of ($8.0 \pm 0.4 \times 10^7$) CFU/mL in the 500 mL PCL triol media. At this stage, 100 mL aliquots of the culture grown in PCL triol media were distributed into each reactor used for biodegradation experiments.

*ii. Biodegradation Setup.* Each reactor (150 mL Erlenmeyer flask) contained a sterile (see SI) CNT/PCL nanocomposite paired with a sterile internal PCL sample (i.e., one nanocomposite coupon and one PCL coupon per reactor). Internal PCL samples were included as part of this study to ensure that PCL biodegradation was occurring consistently in each of the reactors under the conditions used in this study. Four reactors, each containing a nanocomposite at a given CNT loading (paired with an internal PCL sample) were filled with 100 mL aliquots of culture, without washing, from one 500 mL PCL triol/*P. aeruginosa* culture. This process is described in SI Scheme S1. To provide a CNT-free reference for the biodegradation kinetics, three "external" PCL references were biodegraded in separate reactors that *did not* contain CNT/PCL nanocomposites; in contrast, "internal" PCL samples were biodegraded in the same reactors as CNT/PCL nanocomposites.

*iii. Sampling.* Each reactor containing internal PCL and CNT/PCL nanocomposites submerged in PCL triol/*P. aeruginosa* culture was shaken at 125 rpm ± 1 rpm and 28 °C ± 1 °C in two week intervals, conditions that yielded a measurable mass loss of PCL. At the end of each two-week interval, PCL and CNT/PCL samples were collected, washed gently with Milli-Q water, dried for 48 h, and weighed. After weighing, each sample was resterilized with ethanol and resubmerged in 100 mL of freshly prepared PCL triol/*P. aeruginosa* culture for another 2 weeks of biodegradation (details provided in SI). The same procedure was followed for abiotic controls and extracellular enzyme controls. Experiments were carried out for >20 weeks. To assess the effect of sampling time, 0.1% w/w MWCNT/PCL nanocomposites paired with internal PCL references were also exposed to PCL triol/*P. aeruginosa* culture for 4 weeks as described in the SI. The mass loss observed after two and four week periods of incubation is reported in SI Table S2.

*iv. Abiotic and Enzyme Activity Controls.* For abiotic controls, CNT/PCL nanocomposites and internal PCL samples were subjected to the same conditions used for biodegradation (28 °C, 125 rpm, two-week sampling) but were submerged in sterile PCL triol media, to verify that under these conditions, polymer mass loss/dissolution did not occur over the time course of the biodegradation experiment.

The enzyme activity of the *P.aeruginosa*/PCL triol culture was measured initially and after 2 weeks in reactors (100 mL aliquots) which did not contain PCL coupons (SI Table S3). PCL triol was found to be present in the flasks throughout the entire 2 weeks (SI Table S3). Enzyme activity was measured with a Lipase Activity Assay kit II (BioVision, VWR, Radnor, PA) and a 96-well plate spectrophotometer using the supernatant collected after centrifugation of the culture at 4300 rpm for 20 min to remove cells from suspension. Lipase activity is reported in mU/mL. In this assay, one unit of lipase is the amount of enzyme that will generate 1.0 μmol of the product (TNB = 2-nitro-5-thiobenzoate) per minute at 37 °C. Further details about the enzyme activity assay can be found in the SI.

To measure the extent to which extracellular enzymes contributed to PCL decomposition, separate experiments were conducted where the *P. aeruginosa*/PCL triol culture was filtered with a 0.45 μm sterile filter, removing the *P. aeruginosa* cells but allowing extracellular enzymes to pass through. The presence of extracellular lipases in the filtrate was confirmed by the enzyme activity assay (SI Table S3). This filtrate was added to reactors containing PCL coupons and shaken at 28 °C, 225 rpm for 3 days, a time period commonly used in enzymatic decomposition studies of PCL. Separate PCL coupons were exposed to the unfiltered culture, containing both bacteria and extracellular lipases, for the same time period. Mass loss for the PCL coupons exposed to the filtrate (containing only extracellular enzymes) was compared to the PCL mass loss experienced by PCL coupons exposed to *P. aeruginosa* in PCL triol media (SI Table S4). The same procedure was followed for 1% w/w and 10% w/w O-MWCNT/PCL nanocomposites (SI Table S4).


DOI: 10.1021/acs.est.7b02062
Environ. Sci. Technol. 2018, 52, 40−51

**Assessment of Biodegradation Processes.** *i. Scanning Electron Microscopy (SEM).* SEM was used to characterize the surface morphology and CNT distribution at the surface of CNT/PCL nanocomposites before and after biodegradation. Replicate SEM images and imaging procedures are presented in the SI.

*ii. Differential Scanning Calorimetry (DSC).* DSC measurements of PCL, O-MWCNT/PCL, and MWCNT/PCL nanocomposites were taken to measure the fraction of crystallinity, a property that can affect biodegradation rates.[56]

*iii. Thermogravimetric Analysis (TGA).* TGA measurements on ∼5 mg samples of PCL and 10% w/w O-MWCNT/PCL nanocomposites (containing the highest CNT loading) were acquired to ensure that the DCM solvent was not trapped in the samples after drying.

*iv. Planktonic Cell Population Measurements.* The microorganism concentrations (CFU/mL) in sample reactors containing 0.5, 5, and 10% w/w O-MWCNT/PCL nanocomposites were measured using standard plate counting (spread plate method) after a two-week period of biodegradation, corresponding to the interval between weeks 30 and 32 of incubation. These experiments were designed to determine if the presence of the CNT/PCL nanocomposites had an effect on the microbial population in the media.[57]

*v. Biofilm Growth on CNT/PCL Nanocomposites.* In the present study, biofilms on CNT/PCL nanocomposite coupons were imaged with SEM. The effect of CNT incorporation on the characteristics of biofilm formation has previously been studied by our research group using confocal laser scanning microscopy (CLSM) in conjunction with LIVE/DEAD staining.[41] Selected results from these studies, along with the relevant experimental conditions, are also included in the SI (Figure S18) for comparative purposes.

*vi. CNT Release Measurements.* CNT release studies were conducted using 0.1 and 5% w/w MWCNT/PCL nanocomposites containing MWCNTs from Southwest Nanotechnologies Inc. Complete details of these experiments and a description of the MWCNTs can be found in the SI. These MWCNTs contained residual Mo and Co nanoparticles, whose presence could be detected and quantified with single particle ICP-MS (spICP-MS) as a means to track the release of any MWCNTs during biodegradation. The atomic concentrations of metals in the CNTs used in this study were determined with energy dispersive X-ray analysis (SI Table S15).

## RESULTS AND DISCUSSION

Figure 1 (left-hand side) shows SEM images of the as-prepared 0.5 and 10% w/w oxidized MWCNT/PCL nanocomposites. Replicate SEM images of nanocomposites containing several more O-MWCNT loadings and the pristine MWCNT/PCL nanocomposites are shown in SI Figures S2−S12. Visually, the CNT/PNCs are uniformly black and increase in darkness with CNT loading (SI Figure S1). SEM images of both oxidized and pristine MWCNT/PCL nanocomposites show randomly distributed pores with a general increase in CNT concentration at the surface as a function of CNT loading (Figure 1 (left-hand side) and SI Figures S2−S3). In PCL matrices containing pristine MWCNTs, a small number of MWCNT aggregates were observed (see SI Figures S1 and S10 −S12), although the vast majority of CNTs were homogeneously distributed.

The right-hand side of Figure 1 shows SEM images of 0.5 and 10% w/w O-MWCNT/PCL nanocomposites after 32 weeks of biodegradation. For both CNT loadings, PCL

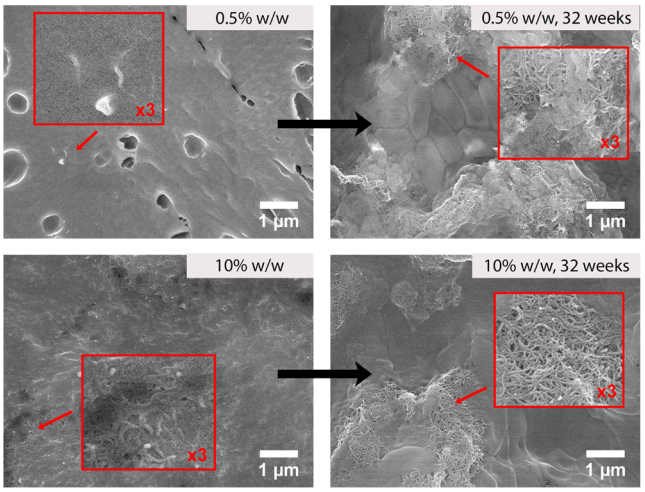


**Figure 1.** SEM images of 0.5 and 10% w/w O-MWCNT/PCL nanocomposites before (left-hand side) and after 32 weeks of biodegradation (right-hand side) with CNT structures magnified in selected areas as indicated by red arrows. Discrete bacterial cells are clearly visible on the surface as well after 32 weeks of biodegradation.

biodegradation leads to CNT accumulation at the surface. Furthermore, both 0.5 and 10% w/w O-MWCNT/PCL surfaces appear similar after biodegradation, with an entangled network of CNTs (delineated by arrows) in regions of the surface not coated by biofilm, which was evidenced in many cases by discrete bacterial cells. Similar replicate SEM images were observed at other O-MWCNT loadings and with pristine MWCNTs (SI Figures S13−S17). CNT accumulation due to the removal of the polymer matrix supports the idea that CNTs are not biodegrading over the time course of PCL biodegradation. The surface accumulation of CNTs during biodegradation is strikingly similar to what has been observed in other environmental transformation processes of CNT/PNCs, including photodegradation and abrasion.[52,58,59]

The relative biodegradation rates of PCL and CNT/PCL nanocomposites by *P. aeruginosa* were determined using mass loss measurements. As described in the experimental section, PCL triol supplement, a soluble form of PCL that was accessible to the microorganisms, was used to accelerate the PCL and CNT/PCL nanocomposite mass loss rate to an experimentally tractable time scale by promoting the growth of lipase-producing *P. aeruginosa* in the media. Over approximately 20 weeks, 100% mass loss of the external PCL references occurred (SI Figure S20). Control studies indicated that PCL mass loss did not occur under abiotic conditions when PCL was exposed to the same media, temperature, shaking speed, and incubation time. Consequently, the mass loss of PCL and CNT/PCL nanocomposites observed in this investigation is attributed to biotic processes.

Figure 2 shows four mass loss plots of oxidized MWCNT/PCL nanocomposites containing 0.5, 2, 5, and 10% w/w O-MWCNTs, represented by solid circles and plotted as a function of incubation time. Each of the four mass loss plots is accompanied by data (open circles) that shows the average mass loss obtained from three external PCL references exposed to *P. aeruginosa* in separate reactors. Since all of the experimental evidence indicates that CNTs are inert to biodegradation over the time scale of this study (32 weeks), mass loss was plotted in terms of the percentage PCL matrix mass loss, as determined by the equation:



DOI: 10.1021/acs.est.7b02062
Environ. Sci. Technol. 2018, 52, 40−51

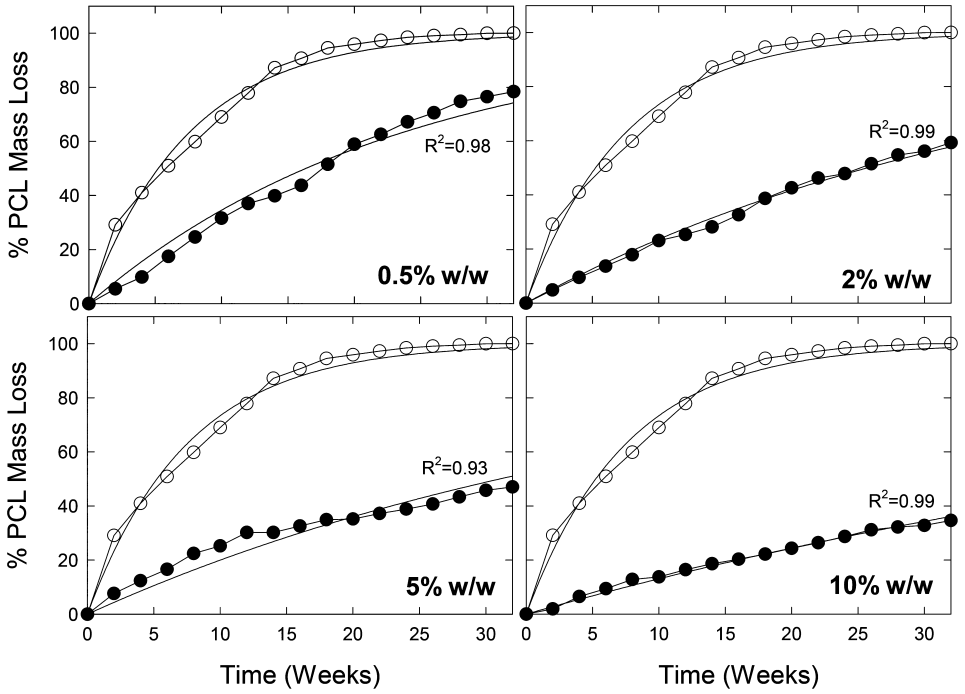


**Figure 2.** Kinetics of PCL matrix mass loss (shown as filled circles) from O-MWCNT/PCL nanocomposites containing 0.5, 2, 5, and 10% w/w O-MWCNTs as a result of *P. aeruginosa* biodegradation in 3 g/L PCL triol/BMM solution. For comparison, each O-MWCNT/PCL mass loss profile is accompanied by the average mass loss from external PCL references (shown as open circles). Mass loss plots of replicate O-MWNCT/PCL nanocomposites at each O-MWCNT loading are presented in the SI. The solid lines in each mass loss profile represent the best fit mass loss profiles using eq 2 (see text for details).

$$\%\text{PCL matrix mass loss} = \frac{\text{PNC mass}_i - \text{PNC mass}_t}{(\text{PNC mass}_i - \text{CNT mass})} \cdot 100 \quad (1)$$

where the numerator is the measured PCL matrix mass loss at time ($t$) of the MWCNT/PCL nanocomposite (PNC) obtained by subtracting the initial ($i$) mass of PNC (PNC mass$_i$) by the PNC mass at a particular time point (PNC mass$_t$). The numerator was then divided by the initial mass of PCL matrix in the PNC (PNC mass$_i$ less the mass of CNTs due to their inherent lack of biodegradability) and multiplied by 100. Mass loss profiles of replicate 0.1 and 1% w/w O-MWCNT/PCL nanocomposites, replicates for 0.5, 2, 5, and 10% w/w O-MWCNT loadings, and abiotic controls are shown in SI Figures S21–S27. Figure 2 shows that *P. aeruginosa* biodegraded the PCL matrix in all O-MWCNT/PCL nanocomposites. However, the rates of polymer biodegradation in O-MWCNT/PCL nanocomposites were less than that of PCL, and decreased with increasing CNT loading. Thus, after 32 weeks of incubation time, the 0.5, 2, 5, and 10% w/w O-MWCNT/PCL nanocomposites lost 78, 59, 47, and 35% PCL matrix mass, respectively (Figure 2).

Three random nanocomposite coupons exhibited significantly lower biodegradation rates compared to other O-MWCNT/PCL nanocomposites with the same O-MWCNT mass loading. These three coupons became tightly rolled during biodegradation (SI Figures S21(d–f)–S22(d–f)), reducing their surface area and therefore their biodegradation rate. These structural changes obscured the effect of CNT inclusion on biodegradation kinetics, and data from these three coupons was therefore not included in our analysis.

In SI Figure S28, CNT/PCL nanocomposites containing pristine MWCNTs with loadings ranging from 0.1 to 5% w/w were biodegraded with *P. aeruginosa*. Similar mass loss trends were observed: (1) all MWCNT/PCL nanocomposites biodegraded at a slower rate than PCL and (2) the rate of mass loss decreased with increasing MWCNT loading. Mass loss plots of 0.5% w/w MWCNT/PCL nanocomposites, replicate mass loss plots of all other CNT mass loadings, and abiotic controls are shown in SI Figures S28–S34.

The reduced biodegradability of CNT/PCL nanocomposites relative to PCL could have been due to an increase in polymer crystallinity caused by the addition of CNTs.[56,60,61] As shown in SI Table S1, the fraction of crystallinity, measured with DSC, did not vary by more than 5% between all of the CNT/PCL nanocomposites studied and did not vary systematically with increasing CNT loading. Therefore, the inhibitory effect of CNTs on PCL biodegradability is not due to any change in the polymer's crystallinity. There was also no evidence of trapped solvent in the nanocomposites (from preparation) contributing to biodegradation inhibition as indicated by the absence of mass loss in the TGA profile at around 104 °C, the boiling point of DCM (SI Figure S19).[62] It is also important to note that the EC surfactant, which enabled homogeneous dispersion of the CNTs in the PCL matrix, was incorporated into all of the CNT/PCL nanocomposites at a consistent mass concentration (4% w/w EC). This prevented crystallinity differences between samples as a result of varying EC content. Moreover, experiments on pure EC samples revealed that there was no EC biodegradation over the duration of our studies (SI Figure S35). Consequently, the use of a consistent EC loading in all CNT/PCL and PCL samples ensured that any changes in PCL matrix biodegradation were due to the CNTs.

The nanocomposites' structural integrity was also visually assessed as biodegradation proceeded. For higher (≥2% w/w) CNT mass loadings (SI Figures S24(c)–S26(c), S32(c)–S33(c)) the nanocomposites circular shape remained unchanged; however, for CNT mass loadings ≤1% w/w, the


DOI: 10.1021/acs.est.7b02062
Environ. Sci. Technol. 2018, 52, 40–51

**a)**

| % O-MWCNT Loading (w/w) | $k_{avg}$ | Std. Dev. k | n |
|---|---|---|---|
| 0 | 0.140 | 0.038 | 3 |
| 0.1 | 0.031 | 0.006 | 3 |
| 0.5 | 0.051 | 0.009 | 2 |
| 1 | 0.044 | 0.011 | 4 |
| 2 | 0.028 | 0.001 | 4 |
| 5 | 0.018 | 0.003 | 4 |
| 10 | 0.015 | 0.001 | 4 |

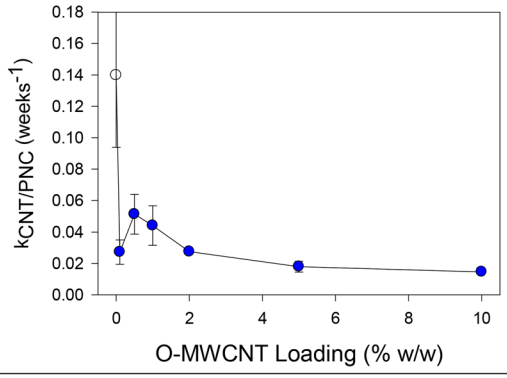


*Mean differences (t) in $k_{avg}$ from student's t-test*

| % O-MWCNT Loading (w/w) | 0 | 0.1 | 0.5 | 1 | 2 | 5 | 10 |
|---|---|---|---|---|---|---|---|
| 0 | - | | | | | | |
| 0.1 | 8.02*** | - | | | | | |
| 0.5 | 5.63*** | 1.54 | - | | | | |
| 1 | 7.29*** | 1.28 | 0.49 | - | | | |
| 2 | 8.55*** | 0.02 | 1.60 | 1.36 | - | | |
| 5 | 9.28*** | 0.71 | 2.25* | 2.15* | 0.79 | - | |
| 10 | 9.53*** | 0.96 | 2.47* | 2.42* | 1.06 | 0.27 | - |

**b)**

| % MWCNT Loading (w/w) | $k_{avg}$ | Std. Dev. k | n |
|---|---|---|---|
| 0 | 0.140 | 0.038 | 3 |
| 0.1 | 0.058 | 0.007 | 4 |
| 0.5 | 0.017 | 0.004 | 4 |
| 1 | 0.031 | 0.004 | 4 |
| 2 | 0.022 | 0.006 | 4 |
| 5 | 0.022 | 0.005 | 4 |

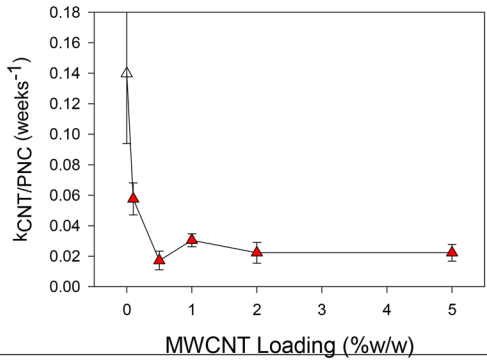


*Mean differences (t) in $k_{avg}$ from student's t-test*

| % MWCNT Loading (w/w) | 0 | 0.1 | 0.5 | 1 | 2 | 5 |
|---|---|---|---|---|---|---|
| 0 | - | | | | | |
| 0.1 | 6.00*** | - | | | | |
| 0.5 | 8.95*** | 3.18** | - | | | |
| 1 | 7.98*** | 2.14* | 1.04 | - | | |
| 2 | 8.58*** | 2.79* | 0.40 | 0.65 | - | |
| 5 | 8.58*** | 2.79* | 0.40 | 0.65 | 0.00 | - |

**Figure 3.** Effect of CNT loading on the biodegradation rate constants for PCL matrix mass loss of (a) *oxidized* MWCNT/PCL (blue circles) and (b) *pristine* MWCNT/PCL nanocomposites (red triangles) relative to unfilled PCL (unfilled circle/triangle). Each rate constant is an average of 2−4 replicates; rate constants shown in the tables were extracted from fits of the mass loss profiles shown in Figures 2 and SI Figure S28, respectively using eq 2 (see text for details). Statistical differences between mass loss rates ($k$) of nanocomposites containing different CNT loadings were determined using the student's $t$ test (*significant at $p < 0.05$; **significant at $p < 0.01$, ***significant at $p < 0.001$).

circular CNT/PCL nanocomposite shape was lost after 20 weeks of biodegradation (SI Figures S21(c)−S23(c), S29(c)−S31(c)). At the higher CNT loadings, it is likely that the CNT/PNCs retained their structure as a result of entanglement and strong van der Waals forces between CNTs. However, when the CNT mass concentration was sufficiently low, the net effect of these interparticle forces appears to have been insufficient to keep the structure intact under the influence of mechanical agitation (shaking at 125 rpm) after a sufficient quantity of the polymer matrix had been removed.

For PCL, oxidized MWCNT/PCL nanocomposites, and pristine MWCNT/PCL nanocomposites, the variation in % PCL matrix mass loss as a function of time could be reasonably well fit ($R^2 > 0.77$, k values reported in SI Tables S5 and S10, statistical comparison of $k$ values in SI Table S6 and S11) by an exponential rise function (Figure 2 and SI Figure S28):

$$y = 100 \times (1 - e^{-kt}) \quad (2)$$

where ($y$) is the % mass loss of the PCL matrix, ($k$) is the first order biodegradation rate constant in weeks$^{-1}$, and ($t$) is the incubation time in weeks. Best-fit lines through the



DOI: 10.1021/acs.est.7b02062
Environ. Sci. Technol. 2018, 52, 40−51

experimental data based on eq 1 for each CNT/PCL nanocomposite are shown as solid lines in Figure 2 and SI Figure S28. A comparison of k values provided a more quantitative means to assess the effect of CNT incorporation on PCL biodegradation ($k$ values in SI Tables S5 and S10, statistical comparison of $k$ values provided in SI Tables S6 and S11). Since the same mathematical relationship was able to describe the biodegradation kinetics of PCL and CNT/PCL nanocomposites, this suggests that CNT inclusion reduces the rate but does not alter the mechanism of biodegradation. The profile is consistent with a degradation process in which the amorphous regions are rapidly degraded during the initial stages while crystalline regions and inaccessible regions of the polymer are degraded slowly in the later stages.[54,63] Similar mass loss profiles during enzymatic decomposition of PCL and MWCNT/PCL nanocomposites at two CNT loadings (1 and 3% w/w) have been observed by Ho et al.[48]

Figure 3 shows the average biodegradation rate constants for CNT/PCL nanocomposites ($k_{CNT/PNC}$) containing (a) oxidized (blue circles) and pristine (red triangles) MWCNTs, plotted as a function of CNT loading; the external PCL references are represented by open symbols. The average biodegradation rate constants and statistical comparisons are also provided in adjacent tables in Figure 3. The external PCL references exhibited an average ($k$) of 0.13 weeks$^{-1}$. In contrast, the O-MWCNT/PCL nanocomposites, exhibited biodegradation rate constants ranging from 0.048 to 0.014 weeks$^{-1}$, for CNT loadings ranging between 0.1 and 10% w/w (Figure 3(a)). Thus, the external PCL references had biodegradation rate constants more than three times greater than any O-MWCNT/PCL nanocomposite ($p$ > 0.001, student's $t$ test). The analogous plot for the nanocomposites containing pristine MWCNTs is also shown in Figure 3(b). Analysis of Figure 3 reveals that oxidation of CNTs prior to biodegradation does not have a significant impact on the effectiveness of CNTs to inhibit polymer biodegradation. Specifically, the trends in biodegradation rate constant as a function of CNT loading were similar despite the presence of ∼4% oxygen on the O-MWCNTs, the difference in lengths (5−20 $\mu$m vs 1.5 $\mu$m for MWCNT and O-MWCNTs, respectively), slight differences in CNT structure (purity and diameter), and differences in manufacturer. This suggests that different types of CNTs will exhibit similar effects on polymer biodegradation kinetics under the same biological conditions. It should be noted that a deviation from the trend of lower biodegradation rates with increasing CNT loading was observed at one CNT loading for both O-MWCNT (0.1% w/w) and pristine MWCNT/PCL (0.5% w/w) nanocomposites (and was not statistically different from high CNT loadings such as 5 and 10% w/w, see SI Tables S6 and S11). These anomalous biodegradation rates could be a consequence of differences in CNT/PNC structural properties at these lower CNT loadings.

Degradation of the CNT/PCL nanocomposites and the paired PCL coupons could be mediated either by enzymes released from microorganisms present in the biofilm that forms on the CNT/PCL nanocomposites (whose formation is observed in this study by SEM and in previous related studies by CLSM in combination with LIVE/DEAD staining[41]) or from the extracellular enzymes present in the media. Our results point to the determinant role of the microorganisms in the biofilm as mediating the biodegradation process. In a control experiment, microorganisms were removed from the initial culture using a 0.45 $\mu$m filter and the filtrate containing extracellular enzymes was poured into reactors containing PCL coupons and incubated for 3 days, a time period commonly used in enzymatic studies.[26,48,64] PCL mass loss as a result of exposure both to the filtrate (containing only extracellular enzymes) and the unfiltered culture were compared after 3 days. In the presence of extracellular enzymes alone, the PCL coupons did not lose any measurable mass, but lost 8 ± 3% (1.23 mg ± 0.4 mg) mass in the presence of the unfiltered culture (SI Table S4). The results obtained for cultures and filtrates containing O-MWCNT/PCL nanocomposites (SI Table S4) also yielded measurable mass loss, with the extent of mass loss decreasing as the O-MWCNT content increased as expected. In the filtrate, the extracellular enzyme activity was measured to be 5× (standard deviation = 3, see SI Table S3) lower due to enzyme loss during filtration. However, if it is assumed that mass loss from PCL and O-MWCNT/PCL nanocomposites is roughly proportional to the extracellular activity, then we would have expected to observe ≈0.25 mg of mass loss. For comparison, we are routinely able to repeatedly measure mass loss as low as 0.11 mg. Moreover, measurable PCL coupon mass loss by lipases typically involves using much higher enzyme activities of *Pseudomonas* lipase XIII around 1500 mU/mL to 15 000 mU/mL (0.1 mg/mL to 1 mg/mL lipase XIII at an activity of ≥15 units/mg, Sigma-Aldrich L9518) at higher temperatures (usually 37 °C) and in the absence of PCL triol.[48,49,64] This is in stark contrast to the orders of magnitude lower enzyme activity in the present study (5.82 ± 0.03 mU/mL for filtrate, 27 ± 17 mU/mL for the unfiltered culture, SI Table S3).

The extent of CNT release from polymer nanocomposites during biodegradation was also studied using spICP-MS. In these experiments, CNT/PCL nanocomposites were prepared with MWCNTs that contained residual molybdenum catalyst nanoparticles, which could be detected as individual pulses using spICP-MS (experimental details provided in the SI). Figure 4(a) and (b) show representative $^{98}$Mo spICP-MS signals recorded from media in which an external PCL reference and a 5% w/w MWCNT/PCL nanocomposite had biodegraded continuously for 8 weeks without sampling, respectively (see SI for details). For 5% w/w MWCNT/PCL nanocomposites, this led to a 5% average mass loss while 0.1% w/w and the external PCL references lost approximately 7% and 20% mass, respectively. Figure 4(a) and 4(b) are qualitatively similar, with only one pulse greater than 20 counts in each spectrum; $^{98}$Mo is present in both backgrounds at similar levels (see Figure 4(d)) as a result of trace Mo in the media. Figure 4(c) shows the spICP-MS signal observed when 1000 ppb MWCNTs were suspended in basal mineral media. In contrast to Figure 4(a) and (b) there is a significant increase in the number of $^{98}$Mo pulses observed with greater than 20 counts in Figure 4(c). Although large pulses (>20 counts) are observed visually, most $^{98}$Mo pulses generated by MWCNTs occur just above the background with values in the 8−15 count range due to the low average $^{98}$Mo content (<0.1% w/w Mo) in the MWCNTs. This is evidenced by the higher "baseline" $^{98}$Mo signal observed in Figure 4(c), as compared to either Figure 4(a) or (b). Consequently, rather than counts of particle-generated pulses, a more quantitative determination of MWCNT release can be obtained by measuring the total $^{98}$Mo counts (sum of each pulse intensity) recorded by spICP-MS over the same time period (60 s) and with a constant dwell time (100 $\mu$s). Prior spICP-MS studies have shown the catalyst metals to be strongly associated with the CNTs and thus the


DOI: 10.1021/acs.est.7b02062
Environ. Sci. Technol. 2018, 52, 40−51

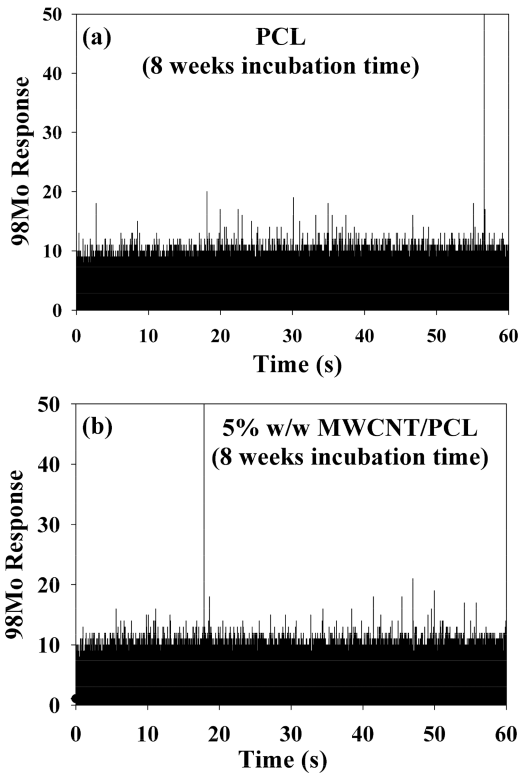


(d)

| Sample | Incubation Time (weeks) | Total $^{98}$Mo Response (counts, x $10^6$) (average of 7-8 replicates) | Standard Deviation (x $10^6$) | RSD (%) |
|---|---|---|---|---|
| PCL | 4 | 2.00 | 0.06 | 3.18 |
| | 8 | 1.95 | 0.07 | 3.67 |
| 0.1% w/w MWCNT/PCL | 4 | 1.88 | 0.06 | 2.94 |
| | 8 | 1.84 | 0.05 | 2.77 |
| 5% w/w MWCNT/PCL | 4 | 1.72 | 0.04 | 2.32 |
| | 8 | 1.82 | 0.09 | 4.80 |

**Figure 4.** Single particle ICP-MS data showing the $^{98}$Mo response from media in which (a) PCL and (b) a 5% w/w MWCNT/PCL nanocomposite had been subjected to 8 weeks of continuous biodegradation; (c) $^{98}$Mo response from BMM with 1000 ppb dispersed MWCNTs added; (d) Total $^{98}$Mo counts obtained from media in which PCL, 0.1% w/w and 5% w/w MWCNT/PCL nanocomposites were biodegraded for 4 and 8 weeks (each data point represents the average of two separate analysis of the media). See text and SI for additional details of sample preparation and analysis.

total metal counts are representative of the CNT mass.[65] Results of the analysis (Figure 4(d)) reveal that there is no statistical or systematic difference between the sum of $^{98}$Mo counts observed for media in which external PCL samples, 0.1% w/w MWCNT/PCL or 5% w/w MWCNT/PCL nanocomposites were subjected to either 4 or 8 weeks of continuous biodegradation. In contrast, calibration experiments where different mass concentrations of MWCNTs were suspended in media revealed that there was the expected linear increase in $^{98}$Mo counts observed as the MWCNT mass concentration increased (see SI Figure S37). Specifically, SI Figure S37 reveals that the release of 500 $\mu$g/L MWCNTs would increase the total number of $^{98}$ Mo counts by $\approx 5.0 \times 10^5$ and also visibly increase the number of pulses having intensities above 20. In comparison, the largest difference in the total number of $^{98}$ Mo counts observed between PCL and the MWCNT/PCL nanocomposites in Figure 4(d) is $4.1 \times 10^5$, with all spICP-MS data exhibiting only a few ($\leq$4) pulses above 20. Therefore, we conclude that the extent of any MWCNT release is <500 $\mu$g/L.

The absence of any detectable MWCNT release is qualitatively consistent with the CNT accumulation observed by SEM during biodegradation of the 5% w/w MWCNT/PCL samples used for CNT release studies (SI Figures S38–S39) and the CNT/PCL nanocomposites used for mass loss studies (Figure 1 and SI Figures S2–S17). CNT release is most likely prevented by the strong van der Waals forces between individual CNTs, as well as CNT entanglement that leads to CNT surface accumulation. However, CNT/PCL nanocomposites of low CNT mass loadings (<1% w/w) eventually lost some of their structural integrity (i.e., circular shape) at later stages of biodegradation (>~60% mass loss, 20 weeks incubation) (SI Figures S21(c)–S23(c), S29(c)–S31(c)). A low CNT density may therefore preclude formation of a stable CNT mat after the polymer matrix is removed, and the possibility of some CNT release from CNT/PCL nanocomposites containing low CNT loadings in the latter stages of biodegradation is possible and worth further investigation.

The experimental data presented in this study clearly shows that the presence of CNTs in the polymer matrix inhibits the rate of PCL biodegradation. A principal reason for this inhibitory effect is ascribed to the cytotoxicity that CNTs embedded in polymer nanocomposites have been shown to exhibit toward *P. aeruginosa*.[33] In previous studies, we have shown that this cytotoxicity is initiated by contact between microorganisms and surface-bound CNTs and is maintained for different types of CNTs, consistent with the inhibitory effect on biodegradation observed in the present study for both pristine and oxidized MWCNTs.[41] Moreover, the degree of cytotoxicity on CNT/PNC surfaces increases with increasing CNT loading, with a functional dependence similar to the one observed in Figure 3 for biodegradation rates.[33] As shown in SI Figure S18, the cytotoxicity of CNTs toward *P. aeruginosa* leads to a "dead" layer of cells forming at the CNT/PNC surface.[41] On top of this "dead" layer of cells, a "living" biofilm develops.[41] The extent of this "dead layer" increases as the CNT content in the PCL increases (see SI Figure S18). To be able to metabolize/biodegrade the PCL carbon source, enzymes associated with the microorganisms of this biofilm must permeate through this dead layer of cells.[41] The presence of this permeation barrier of dead cells (which is a consequence of the cytotoxicity of the CNTs), along with the physical barrier which results from the


DOI: 10.1021/acs.est.7b02062
Environ. Sci. Technol. 2018, 52, 40–51

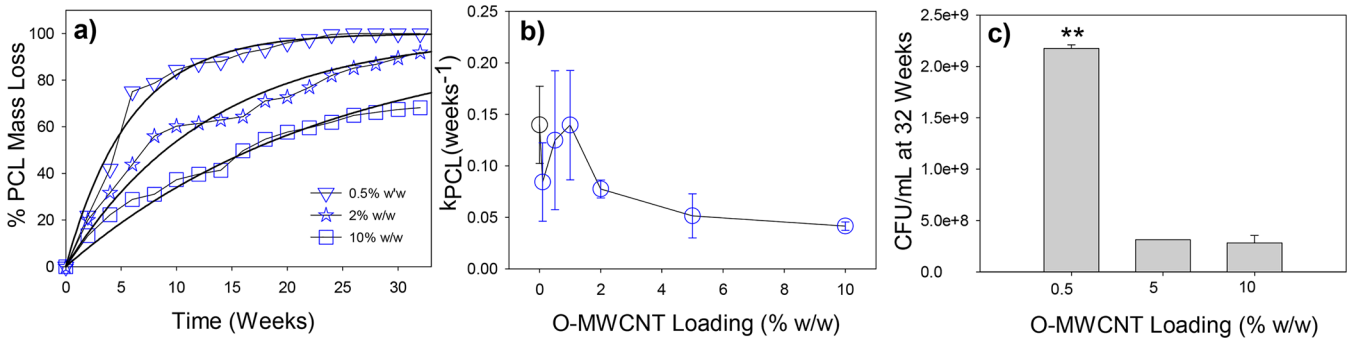


**Figure 5.** (a) Mass loss profiles of internal PCL references paired with O-MWCNT/PCL nanocomposites containing 0.5% w/w (triangles), 2% w/w (stars) and 10% w/w (squares) O-MWCNTs. Solid lines represent best fit lines obtained using eq 2. All biodegradation experiments were a result of exposure to *P. aeruginosa* in 3 g/L PCL triol/BMM solution. Mass loss plots of replicate and other internal PCL samples are presented in the SI. (b) The effect of CNT loading in O-MWCNT/PCL nanocomposites on the biodegradation rate constant of the paired internal PCL samples. Rate constants were determined by fitting the mass loss profiles to eq 2. Values shown are the average plus one standard deviation of 2−4 replicates. Statistically significant differences were assessed with the student's *t* test and are shown in the SI. (c) The CFU in cultures exposed to media containing 0.5, 5, and 10% w/w O-MWCNT/PCL nanocomposites for 2 weeks, in the interval corresponding to the incubation time from 30 to 32 weeks shown in Figure 2. Each measured CFU is the average value of three replicate cultures, each exposed to a reactor containing an internal PCL sample and an O-MWCNT/PCL nanocomposite of the same O-MWCNT loading. Statistical differences between CFU/mL for nanocomposites at each CNT loading were determined using the student's *t* test (*significant at $p < 0.05$; **significant at $p < 0.01$, ***significant at $p < 0.001$). A table with further information and CFU/mL for 1% w/w O-MWCNT/PCL is provided in the SI.

accumulation of CNTs at the surface is ascribed to the decreased rate of PCL biodegradation in the presence of CNTs. As the CNT content in the PCL increases, the scale of this "dead" layer and the quantity of CNTs which accumulate at the surface both increase, resulting in a systematic decrease in the biodegradation rate contrast. In contrast to the effect of CNTs, nanoclay fillers have been shown to promote biodegradation processes, an effect ascribed to an increase in the number of amorphous zones formed at the interface of the filler and the polymer matrix.[23] Since this same effect is likely to occur in CNT/polymer nanocomposites as well, the difference in behavior between these two classes of nanomaterials toward polymer biodegradation further supports the idea that the cytotoxicity of CNTs is important.

In addition to the external PCL references that were biodegraded in separate reactors, each CNT/PCL nanocomposite was paired with a PCL sample in the same reactor. Mass loss plots of these internal PCL samples, paired with oxidized MWCNT/PCL nanocomposites of increasing CNT loading (0.5, 5, and 10% w/w) are shown in Figure 5(a). Analogous mass loss data obtained for the internal PCL samples paired with other O-MWCNT replicates and mass loadings are plotted in SI Figures S21(b)−S26(b). Analysis of Figure 5(a) shows that the internal PCL samples nominally lost mass at a decreasing rate as the % w/w of oxidized or pristine MWCNTs in the companion CNT/PCL nanocomposites increased. Thus, Figure 5(a) shows that after 10 weeks, internal PCL samples in the reactor containing 0.5% w/w O-MWCNT/PCL samples had lost 70% ± 20% mass ($N = 2$), while over the same time period, internal PCL samples in the reactor containing 10% w/w O-MWCNT/PCL samples had lost 35% ± 2% mass ($N = 4$). This nominal trend ($p > 0.05$ with the student *t* test, Table S8) is shown more quantitatively in Figure 5(b) and SI Table S7, using biodegradation rate constants ($k$) obtained by fitting the mass loss profiles shown in SI Figures S21(b)−S26(b) to eq 2; these rate constants are plotted as a function of the O-MWCNT loading in the companion O-MWCNT/PCL nanocomposites. A comparison of Figures 3 and 5(b) reveals that the biodegradation rate constants for O-MWCNT/PCL nanocomposites and for the paired internal PCL samples, respectively, exhibit a similar functional dependence on the O-MWCNT loading. However, the absolute value of the biodegradation rate constants for the internal PCL samples was always greater than the companion O-MWCNT/PCL nanocomposites (SI Table S9 for statistical comparisons of O-MWCNT/PCL nanocomposites to their paired internal PCL samples). For example, after 32 weeks of biodegradation 10% w/w O-MWCNT/PCL nanocomposites had, on average, lost 34 ± 2% PCL matrix mass ($k_{CNT/PNC} = 0.041 \pm 0.003$ weeks$^{-1}$), while the companion internal PCL samples they were paired with had lost 71 ± 4% ($k = 0.015 \pm 0.001$ weeks$^{-1}$, statistically different with the student's *t* test ($t = 12.06$, $p = 0.001$)). The same trend was observed for PCL samples paired with pristine MWCNT/PCL nanocomposites (SI Figures S29(b)−S33(b), Tables S12, S13, and S14 for $k$ values and statistical comparisons; compare Figure 5(b) and SI Figure S36).

Studies were also conducted to explore the effect that the CNT/PCL nanocomposites had on the planktonic microbial population in the media surrounding the nanocomposites. In these experiments, the CFU count was determined for cultures that were exposed to 0.5, 5, and 10% w/w O-MWCNT/PCL nanocomposites for a two-week time period during weeks 30−32 of incubation with *P. aeruginosa* (Figure 2). Initially, the microbial population in all reactors was ($8.0 \pm 0.4 \times 10^7$) CFU and increased to higher values as the microorganisms consumed the PCL matrix over the course of 2 weeks (Figure 5(c)). However, Figure 5(c) and SI Table S17 show that the extent of microbial proliferation was significantly reduced in the presence of CNT/PCL nanocomposites, decreasing from ($2.20 \times 10^9 \pm 0.04 \times 10^9$) CFU to ($2.8 \times 10^8 \pm 0.7 \times 10^8$) CFU as the CNT loading in the CNT/PCL nanocomposite increased from 0.5 to 10% w/w, respectively ($p > 0.01$, student's *t* test, see SI Table S18). This decrease in the suspended microbial population is ascribed to the decreasing biodegradation rates observed for PCL coupons paired with CNT/PCL nanocomposites of increasing CNT mass loading.

Suspended CNTs have previously been shown to exhibit cytotoxicity, but only at a CNT concentration in the 50 mg/L range, a concentration well above the upper bound of ≈500


DOI: 10.1021/acs.est.7b02062
*Environ. Sci. Technol.* 2018, 52, 40−51

μg/L MWCNTs that might have released in this study, as indicated by spICP-MS measurements (see Figure 4).[66] Consequently, the decrease in suspended microbial population observed in Figure 5(c) indicates that there must be a dynamic interplay/equilibrium between microorganisms in the surrounding media and microorganisms associated with the CNT/PCL nanocomposites. Calculations of carbon mass gain as planktonic cells (described in SI Table S19) compared to the carbon mass lost from coupons (SI Table S16) indicate that PCL triol is the principal carbon source used by the planktonic cells to proliferate. Consequently, the data suggests that the proliferation of planktonic cells occurs as a result of cells associating with (and subsequently disassociating from) the biofilm during the growth process while using the PCL triol as the primary food source. The ability of cells to proliferate in such a process would be expected to be negatively impacted by the presence of cytotoxic CNTs at the nanocomposite surface (see Figure 5(c)), as evidenced by the decrease in the fraction of living cells present in the biofilm as the CNT content increases (see SI Figure S18).

## ■ ENVIRONMENTAL IMPLICATIONS

One of the key findings in this study is that the addition of even low mass concentrations of CNTs can significantly impact a polymer's biodegradability with a consequent increase in the polymer's lifetime/persistence. If we operationally define complete biodegradation to be >95% mass loss of PCL, then eq 2 indicates that the presence of 0.5, 2, 5, and 10% w/w O-MWCNTs would cause biodegradation to take 1.1, 2.1, 3.2, and 3.9 years as compared to the ≈5 months it would take PCL. Similarly, pristine MWCNT/PCL nanocomposite biodegradation would take 1.0, 1.9, and 2.6 years for 0.1, 1, and 5% w/w, respectively. It is important to note that our data indicates that the presence of CNTs in polymer matrices retards, but does not prevent biodegradation of the polymer matrix, at least under the conditions of this monoculture study. In terms of the fate of CNTs, no detectable CNT release was observed (<500 μg/L) during biodegradation, although CNTs accumulated at the surface. For all but the lowest CNT loadings, biodegradation ultimately leads to the formation of an interconnected CNT network (mat) as the polymer is metabolized. The impact of the CNT fillers on their surroundings was evidenced by decreased planktonic cell proliferation and a reduced rate of biodegradation for PCL coupons paired in the same reactor as CNT/PCL coupons. Biodegradation of CNT/PNCs under more complex, environmentally relevant (albeit less controlled) mixed culture conditions will provide further insight into the transformation of CNT/PNCs in soils, surface waters, and wastewater treatment plants. In mixed cultures, the presence of CNTs may have less of an impact on polymer biodegradation due to the synergistic metabolic pathways available.

## ■ ASSOCIATED CONTENT

### Supporting Information

The Supporting Information is available free of charge on the ACS Publications website at DOI: 10.1021/acs.est.7b02062.

Images of PCL and CNT/PCL nanocomposite coupons (Figure S1) as well as preparation procedures; further information on biodegradation experiments and a schematic of the biodegradation experiment setup (SI - Scheme S1); SEM analysis and images of CNT/PCL nanocomposites before and after biodegradation (Figures S2- S17); confocal laser scanning microscopy images of LIVE/DEAD stained biofilms grown on neat PCL, on a 0.5% w/w O-MWCNT/PCL nanocomposite under low shear conditions, and on 2% w/w O-MWCNT/PCL nanocomposites under two different conditions (Figure S18); TGA characterization of selected coupons (Figure S19); a comparison of 0.1% w/w MWCNT/PCL nanocomposite mass loss after 2 and 4 weeks of biodegradation (Table S2); extracellular enzyme activity results and statistical comparisons of initial cultures, two-week cultures, and filtrates (Table S3); mass loss results from external PCL references and O-MWCNT/PCL nanocomposites (1% w/w and 10% w/w O-MWCNT loading) submerged in culture versus filtrate for 3 d with statistical comparisons (Table S4); external PCL mass loss plots (Figure S20); CNT/PCL nanocomposite mass loss plots, paired internal PCL mass loss plots, pictures, abiotic controls, outlier samples for O-MWCNT/PCL (Figures S21 − S27) and pristine MWCNT/PCL nanocomposites (Figures S28 − S34); CNT/PCL nanocomposite biodegradation rate constants and statistical comparisons for different CNT loadings, internal PCL sample rate constants and statistical comparisons for internal PCL samples paired to nanocomposites at different CNT loadings, and statistical comparisons between nanocomposites and the internal PCL samples they were paired with for O-MWCNT/PCL (Tables S5 − S9) and pristine MWCNT/PCL nanocomposites (Tables S10 − S14); DSC analysis and crystallinity data for O-MWCNT/PCL nanocomposites as a function of O-MWCNT loading (Table S1); an EC mass loss plot (Figure S35); a plot of the rate constants for internal PCL samples paired to pristine MWCNT/PCL nanocomposites (Figure S36); further data on CNT release (Figure S37); EDS of MWCNTs used in this study (Table S15); SEM images of 5% w/w MWCNT/PCL nanocomposites used for CNT release studies (Figures S38 − S39); calculations and values obtained for carbon mass lost from the nanocomposite coupons (Table S16), CFU/mL values for planktonic cell growth in the culture surrounding nanocomposites after 2 weeks exposure with statistical comparisons (Table S17 and S18); and carbon mass gain calculations of planktonic cells in the culture surrounding the nanocomposites (Table S19) for comparison to the carbon mass lost from the coupons (PDF)

## ■ AUTHOR INFORMATION


### Corresponding Author

*Phone: (410) 516-4328; e-mail: howardf@jhu.edu.

### ORCID

D. Howard Fairbrother: 0000-0003-4405-9728


### Notes

The authors declare no competing financial interest.

## ■ ACKNOWLEDGMENTS

We acknowledge NSF grants CBET #1236493 and CBET #1336168 as well as JHU for an Owens Graduate Fellowship awarded to DGG. The authors would like to thank Kris Marsh, Roderick Go, Julianne Payne, Pat Geronimo, Laila Nasr, and



DOI: 10.1021/acs.est.7b02062
Environ. Sci. Technol. 2018, 52, 40−51

Putarut Sunthranand for their contributions as well as David Durkin for help with TGA and DSC analysis.

## REFERENCES


(1) Du, J.-H.; Bai, J.; Cheng, H. M. The present status and key problems of carbon nanotube based polymer composites. *Express Polym. Lett.* **2007**, *5*, 253−272.

(2) Coleman, J. N.; Khan, U.; Blau, W. J.; Gun'ko, Y. K. Small but strong: A review of the mechanical properties of carbon nanotube-polymer composites. *Carbon* **2006**, *44* (9), 1624−1652.

(3) De, V. M. F. L.; Tawfick, S. H.; Baughman, R. H.; Hart, A. J. Carbon Nanotubes: Present and Future Commercial Applications. *Science* **2013**, *339* (6119), 535−539.

(4) Nanocyl Biocyl. http://www.nanocyl.com/kr/Products-Solutions/Products/BIOCYL (accessed 11 December 2016).

(5) Harrison, B. S.; Atala, A. Carbon nanotube applications for tissue engineering. *Biomaterials* **2007**, *28* (2), 344−353.

(6) Gottschalk, F.; Nowack, B. The release of engineered nanomaterials to the environment. *J. Environ. Monit.* **2011**, *13* (5), 1145−1155.

(7) Petersen, E. J.; Zhang, L. W.; Mattison, N. T.; O'Carroll, D. M.; Whelton, A. J.; Uddin, N.; Nguyen, T.; Huang, Q. G.; Henry, T. B.; Holbrook, R. D.; Chen, K. L. Potential release pathways, environmental fate, and ecological risks of carbon nanotubes. *Environ. Sci. Technol.* **2011**, *45* (23), 9837−9856.

(8) Luckachan, G. E.; Pillai, C. K. S. Biodegradable Polymers-A Review on Recent Trends and Emerging Perspectives. *J. Polym. Environ.* **2011**, *19* (3), 637−676.

(9) Shah, A. A.; Hasan, F.; Hameed, A.; Ahmed, S. Biological degradation of plastics: A comprehensive review. *Biotechnol. Adv.* **2008**, *26* (3), 246−265.

(10) Massardier-Nageotte, V.; Pestre, C.; Cruard-Pradet, T.; Bayard, R. Aerobic and anaerobic biodegradability of polymer films and physico-chemical characterization. *Polym. Degrad. Stab.* **2006**, *91* (3), 620−627.

(11) Madigan, M. T.; Martinko, J. M.; Dunlap, P. V.; Clark, D. P. *Brock Biology of Microorganisms*. 12th ed.; Pearson: San Francisco, 2009.

(12) International, A., ASTM Standard D6954-04. In *Standard Guide for Exposing and Testing Plastics that Degrade in the Environment by a Combination of Oxidation and Biodegradation*, 2013.

(13) International, A., ASTM Standard D7473-12. In *Standard Test Method for Weight Attrition of Plastic Materials in the Marine Environment by Open System Aquarium Incubations*, 2012.

(14) Tokiwa, Y.; Calabia, B. P.; Ugwu, C. U.; Alba, S. Biodegradability of Plastics. *Int. J. Mol. Sci.* **2009**, *10* (9), 3722−3742.

(15) Jones, P. H.; Prasad, D.; Heskins, M.; Morgan, M. H.; Guillet, J. E. Biodegradability of photodegraded polymers. I. Development of experimental procedures. *Environ. Sci. Technol.* **1974**, *8* (10), 919−923.

(16) Gross, R. A.; Kalra, B. Biodegradable Polymers for the Environment. *Science* **2002**, *297*, 803−807.

(17) Shih, Y. F.; Chen, L. S.; Jeng, R. J. Preparation and properties of biodegradable PBS/multi-walled carbon nanotube nanocomposites. *Polymer* **2008**, *49* (21), 4602−4611.

(18) Jayasekara, R.; Sheridan, S.; Lourbakos, E.; Beh, H.; Christie, G. B. Y.; Jenkins, M.; Halley, P. B.; McGlashan, S.; Lonergan, G. T. Biodegradation and ecotoxicity evaluation of a bionolle and starch blend and its degradation products in compost. *Int. Biodeterior. Biodegrad.* **2003**, *51* (1), 77−81.

(19) Benedict, C. V.; Cameron, J. A.; Huang, S. J. Polycaprolactone degradation by mixed and pure cultures of bacteria and a yeast. *J. Appl. Polym. Sci.* **1983**, *28* (1), 335−342.

(20) Posen, I. D.; Jaramillo, P.; Griffin, W. M. Uncertainty in the Life Cycle Greenhouse Gas Emissions from U.S. Production of Three Biobased Polymer Families. *Environ. Sci. Technol.* **2016**, *50* (6), 2846−2858.

(21) Mittal, V. *Nanocomposites with Biodegradable Polymers: Synthesis, Properties, and Future Perspectives*; Oxford University Press, 2011.

(22) Kumar, S.; Maiti, P. Understanding the controlled biodegradation of polymers using nanoclays. *Polymer* **2015**, *76*, 25−33.

(23) Singh, N. K.; Das Purkayastha, B.; Roy, J. K.; Banik, R. M.; Yashpal, M.; Singh, G.; Malik, S.; Maiti, P. Nanoparticle-Induced Controlled Biodegradation and Its Mechanism in Poly(epsilon-caprolactone). *ACS Appl. Mater. Interfaces* **2010**, *2* (1), 69−81.

(24) Balkova, R.; Hermanova, S.; Voberkova, S.; Damborsky, P.; Richtera, L.; Omelkova, J.; Jancar, J. Structure and morphology of microbial degraded poly (ε-caprolactone)/graphite oxide composite. *J. Polym. Environ.* **2014**, *22* (2), 190−199.

(25) Fan, J.; Grande, C. D.; Rodrigues, D. F. Biodegradation of graphene oxide-polymer nanocomposite films in wastewater. *Environ. Sci.: Nano* **2017**, *4*, 1808.

(26) Singh, N. K.; Singh, S. K.; Dash, D.; Gonugunta, P.; Misra, M.; Maiti, P. CNT Induced beta-Phase in Polylactide: Unique Crystallization, Biodegradation, and Biocompatibility. *J. Phys. Chem. C* **2013**, *117* (19), 10163−10174.

(27) Kumar, S.; Maiti, P. Controlled biodegradation of polymers using nanoparticles and its application. *RSC Adv.* **2016**, *6* (72), 67449−67480.

(28) Fukushima, K.; Abbate, C.; Tabuani, D.; Gennari, M.; Rizzarelli, P.; Camino, G. Biodegradation trend of poly (ε-caprolactone) and nanocomposites. *Mater. Sci. Eng., C* **2010**, *30* (4), 566−574.

(29) Lefevre, C.; Tidjani, A.; Vander, W. C.; David, C. The interaction mechanism between microorganisms and substrate in the biodegradation of polycaprolactone. *J. Appl. Polym. Sci.* **2002**, *83* (6), 1334−1340.

(30) Bianco, A.; Kostarelos, K.; Prato, M. Making carbon nanotubes biocompatible and biodegradable. *Chem. Commun.* **2011**, *47* (37), 10182−10188.

(31) Russier, J.; Menard-Moyon, C.; Venturelli, E.; Gravel, E.; Marcolongo, G.; Meneghetti, M.; Doris, E.; Bianco, A. Oxidative biodegradation of single-and multi-walled carbon nanotubes. *Nanoscale* **2011**, *3* (3), 893−896.

(32) Zhang, L.; Petersen, E. J.; Habteselassie, M. Y.; Mao, L.; Huang, Q. Degradation of multiwall carbon nanotubes by bacteria. *Environ. Pollut. (Oxford, U. K.)* **2013**, *181*, 335−339.

(33) Goodwin, D. G.; Marsh, K. M.; Sosa, I. B.; Payne, J. B.; Gorham, J. M.; Bouwer, E. J.; Fairbrother, D. H. Interactions of Microorganisms with Polymer Nanocomposite Surfaces Containing Oxidized Carbon Nanotubes. *Environ. Sci. Technol.* **2015**, *49* (9), 5484−5492.

(34) Ahmed, F.; Santos, C. M.; Vergara, R. A. M. V.; Tria, M. C. R.; Advincula, R.; Rodrigues, D. F. Antimicrobial applications of electroactive PVK-SWNT nanocomposites. *Environ. Sci. Technol.* **2012**, *46* (3), 1804−1810.

(35) Santos, C. M.; Milagros Cui, K.; Ahmed, F.; Tria, M. C. R.; Vergara, R. A. M. V.; de Leon, A. C.; Advincula, R. C.; Rodrigues, D. F. Bactericidal and anticorrosion properties in PVK/MWNT nanocomposite coatings on stainless steel. *Macromol. Mater. Eng.* **2012**, *297* (8), 807−813.

(36) Schiffman, J. D.; Elimelech, M. Antibacterial activity of electrospun polymer mats with incorporated narrow diameter single-walled carbon nanotubes. *ACS Appl. Mater. Interfaces* **2011**, *3* (2), 462−468.

(37) Shimao, M. Biodegradation of plastics. *Curr. Opin. Biotechnol.* **2001**, *12* (3), 242−247.

(38) Mattioli-Belmonte, M.; Vozzi, G.; Whulanza, Y.; Seggiani, M.; Fantauzzi, V.; Orsini, G.; Ahluwalia, A. Tuning polycaprolactone-carbon nanotube composites for bone tissue engineering scaffolds. *Mater. Sci. Eng., C* **2012**, *32* (2), 152−159.

(39) Chakoli, A. N.; Wan, J.; Feng, J. T.; Amirian, M.; Sui, J. H.; Cai, W. Functionalization of multiwalled carbon nanotubes for reinforcing of poly(-lactide-co-ε-caprolactone) biodegradable copolymers. *Appl. Surf. Sci.* **2009**, *256* (1), 170−177.

(40) Pan, L.; Pei, X.; He, R.; Wan, Q.; Wang, J. Multiwall carbon nanotubes/polycaprolactone composites for bone tissue engineering application. *Colloids Surf., B* **2012**, *93*, 226−234.




DOI: 10.1021/acs.est.7b02062
*Environ. Sci. Technol.* 2018, 52, 40−51

(41) Goodwin, D. G.; Xia, Z.; Gordon, T.; Gao, C.; Bouwer, E.; Fairbrother, D. Biofilm development on carbon nanotube/polymer nanocomposites. *Environ. Sci.: Nano* **2016**, *3* (3), 545−558.
(42) Kale, S. K.; Deshmukh, A. G.; Dudhare, M. S.; Patil, V. B. Microbial degradation of plastic: A review. *Journal of Biochemical Technology* **2015**, *6* (2), 952−961.
(43) Mohan, S. V.; Kisa, T.; Ohkuma, T.; Kanaly, R. A.; Shimizu, Y. Bioremediation technologies for treatment of PAH-contaminated soil and strategies to enhance process efficiency. *Rev. Environ. Sci. Bio/Technol.* **2006**, *5* (4), 347−374.
(44) Hasan, F.; Shah, A. A.; Hameed, A. Industrial applications of microbial lipases. *Enzyme Microb. Technol.* **2006**, *39* (2), 235−251.
(45) Khatiwala, V. K.; Shekhar, N.; Aggarwal, S.; Mandal, U. K. Biodegradation of Poly(ε-caprolactone) (PCL) film by Alcaligenes faecalis. *J. Polym. Environ.* **2008**, *16* (1), 61−67.
(46) Li, S.; Garreau, H.; Pauvert, B.; McGrath, J.; Toniolo, A.; Vert, M. Enzymatic Degradation of Block Copolymers Prepared from ε-Caprolactone and Poly(ethylene glycol). *Biomacromolecules* **2002**, *3* (3), 525−530.
(47) Qiu, Z.; Wang, H.; Xu, C. Crystallization, mechanical properties, and controlled enzymatic degradation of biodegradable poly(ε-caprolactone)/multi-walled carbon nanotubes nanocomposites. *J. Nanosci. Nanotechnol.* **2011**, *11*, 7884−7893.
(48) Ho, C. M. B.; Mishra, A.; Lin, P. T. P.; Ng, S. H.; Yeong, W. Y.; Kim, Y. J.; Yoon, Y. J. 3D Printed Polycaprolactone Carbon Nanotube Composite Scaffolds for Cardiac Tissue Engineering. *Macromol. Biosci.* **2017**, *17* (4), 1600250.
(49) Pawar, S. P.; Kumar, S.; Misra, A.; Deshmukh, S.; Chatterjee, K.; Bose, S. Enzymatically degradable EMI shielding materials derived from PCL based nanocomposites. *RSC Adv.* **2015**, *5* (23), 17716−17725.
(50) Zeng, H. L.; Gao, C.; Yan, D. Y. Poly(ϵ-caprolactone)-Functionalized Carbon Nanotubes and Their Biodegradation Properties. *Adv. Funct. Mater.* **2006**, *16* (6), 812−818.
(51) Lankone, R. S.; Wang, J.; Ranville, J. F.; Fairbrother, D. H. Photodegradation of polymer-CNT nanocomposites: effect of CNT loading and CNT release characteristics. *Environ. Sci.: Nano* **2017**, *4* (4), 967−982.
(52) Petersen, E. J.; Lam, T.; Gorham, J. M.; Scott, K. C.; Long, C. J.; Stanley, D.; Sharma, R.; Alexander Liddle, J.; Pellegrin, B.; Nguyen, T. Methods to assess the impact of UV irradiation on the surface chemistry and structure of multiwall carbon nanotube epoxy nanocomposites. *Carbon* **2014**, *69*, 194−205.
(53) Reed, R. B.; Goodwin, D. G.; Marsh, K. L.; Capracotta, S. S.; Higgins, C. P.; Fairbrother, D. H.; Ranville, J. F. Detection of single walled carbon nanotubes by monitoring embedded metals. *Environ. Sci.: Processes Impacts* **2013**, *15* (1), 204−213.
(54) Khatiwala, V. K.; Shekhar, N.; Aggarwal, S.; Mandal, U. Biodegradation of poly (ε-caprolactone)(PCL) film by Alcaligenes faecalis. *J. Polym. Environ.* **2008**, *16* (1), 61−67.
(55) Oda, Y.; Oida, N.; Urakami, T.; Tonomura, K. Polycaprolactone depolymerase produced by the bacterium Alcaligenes faecalis. *FEMS Microbiol. Lett.* **1997**, *152* (2), 339−343.
(56) Zhang, S.; Li, L.; Kumar, A. *Materials Characterization Techniques*; CRC press, 2008.
(57) Harley, J. P. *Laboratory Exercises in Microbiology*; McGraw-Hill Science Engineering, 2004.
(58) Nguyen, T.; Pellegrin, B.; Mermet, L.; Shapiro, A.; Gu, X.; Chin, J. Network aggregation of CNTs at the surface of epoxy/MWCNT composite exposed to UV radiation. *Nanotechnology* **2009**, *1*, 90−3.
(59) Kim, J. Y.; Park, H. S.; Kim, S. H. Thermal decomposition behavior of carbon-nanotube-reinforced poly (ethylene 2, 6-naphthalate) nanocomposites. *J. Appl. Polym. Sci.* **2009**, *113* (3), 2008−2017.
(60) Sobkowicz, M. J.; Sosa, R.; Dorgan, J. R. Supramolecular bionanocomposites, part 2: Effects of carbon nanoparticle surface functionality on polylactide crystallization. *J. Appl. Polym. Sci.* **2011**, *121* (4), 2029−2038.
(61) Hakkarainen, M.; Albertsson, A. C. Heterogeneous biodegradation of polycaprolactone−low molecular weight products and surface changes. *Macromol. Chem. Phys.* **2002**, *203* (10−11), 1357−1363.
(62) O'Neil, M. J. *The Merck Index: An Encyclopedia of Chemicals, Drugs, And Biologicals*; RSC Publishing, 2013.
(63) Lefevre, C.; Tidjani, A.; Vander Wauven, C.; David, C. The interaction mechanism between microorganisms and substrate in the biodegradation of polycaprolactone. *J. Appl. Polym. Sci.* **2002**, *83* (6), 1334−1340.
(64) Singh, N. K.; Purkayastha, B. D.; Roy, J. K.; Banik, R. M.; Yashpal, M.; Singh, G.; Malik, S.; Maiti, P. Nanoparticle-induced controlled biodegradation and its mechanism in poly (ε-caprolactone). *ACS Appl. Mater. Interfaces* **2009**, *2* (1), 69−81.
(65) Wang, J.; Lankone, R. S.; Reed, R. B.; Fairbrother, D. H.; Ranville, J. F. Analysis of single-walled carbon nanotubes using spICP-MS with microsecond dwell time. *NanoImpact* **2016**, *1*, 65−72.
(66) Arias, L. R.; Yang, L. Inactivation of Bacterial Pathogens by Carbon Nanotubes in Suspensions. *Langmuir* **2009**, *25* (5), 3003−3012.


DOI: 10.1021/acs.est.7b02062
*Environ. Sci. Technol.* 2018, 52, 40−51